Chinese Chemical Letters 33 (2022) 1259–1262

Contents lists available at ScienceDirect

Chinese Chemical Letters

journal homepage: www.elsevier.com/locate/cclet

Highly efficient photocatalytic NO removal and *in situ* DRIFTS investigation on $SrSn(OH)_6$

Wendong Zhang[a,*], Yun Wang[a], Yi Wang[a], Yi Liang[a], Fan Dong[b,c,*]

[a] *Chongqing Key Laboratory of Inorganic Functional Materials, Chongqing Key Laboratory of Green Synthesis and Application, Chongqing Normal University, Chongqing 401331, China*

[b] *Yangtze Delta Region Institute (Huzhou) & Institute of Fundamental and Frontier Sciences, University of Electronic Science and Technology of China, Huzhou 313001, China*

[c] *State Centre for International Cooperation on Designer Low-carbon and Environmental Materials (CDLCEM), School of Materials Science and Engineering, Zhengzhou University, Zhengzhou 450001, China*

ARTICLE INFO

Article history:
Received 23 March 2021
Revised 4 June 2021
Accepted 28 July 2021
Available online 5 August 2021

Keywords:
Highly efficient
NO removal
In situ DRIFTS investigation
$SrSn(OH)_6$;
Reaction mechanism

ABSTRACT

A novel $SrSn(OH)_6$ photocatalyst with large plate and particle size were synthesized *via* a facile chemical precipitation method. The photocatalytic activity of the $SrSn(OH)_6$ was evaluated by the removal of NO at ppb level under UV light irradiation. Based on the ESR measurements, $SrSn(OH)_6$ photocatalyst was found to have the ability to generate the main active species of $O_2^{\bullet-}$, $^{\bullet}OH$ and $^1O_2$ during the photocatalytic process. Moreover, $SrSn(OH)_6$ photocatalyst not only exhibits high photocatalytic activity for NO removal (79.6%), but also has good stability after five cycles. The *in situ* diffuse reflectance infrared Fourier transform spectroscopy (DRIFTS) was used to investigate the NO_x transfer pathway and the intermediate products distribution during the adsorption and photocatalytic NO oxidation process. The present work not only provides an efficient material for air pollutants purification at room temperature but also in-depth understanding of the mechanism involved in the photocatalytic NO removal process.

Air pollution is one of the most serious environmental issues, which results in extremely hazardous effects and risks on public health and ecological security [1,2]. However, conventional methods including physical, chemical and biological methods are difficult to remove the low-concentration of air pollutants (such as nitrogen oxide (NO_x), volatile organic compounds (VOCs), *etc.*) [3,4]. Furthermore, most of the above-mentioned methods have disadvantages of requiring complicated techniques, harsh conditions, high costs and time consuming, which greatly limit their practical application. Hence, it is highly desirable to develop a green, stable and efficient method to improve air quality.

Photocatalysis is considered as a promising method for air pollutants purification that needs only photocatalyst, sunlight, O_2 and H_2O [5,6]. Over the past few decades, many attempts have been made to develop a large amount of photocatalysts for the field of environmental remediation, including metal-based photocatalysts (*e.g.*, TiO_2, $Bi_4O_5Br_2$, $SrTiO_3$, $(BiO)_2CO_3$, Ag_3PO_4, WS_2, Au/TiO_2 and Ag/AgCl) [7-10], polymeric photocatalysts (*e.g.*, g-C_3N_4, poly(diphenylbutadiyne), and polyimide) [11-13], and elemental-based photocatalysts (*e.g.*, Bi, Bi/TiO_2, S, and P) [14-16]. However, most of the above-mentioned photocatalysts are still far from satisfactory because of their low sunlight harvesting ability, high charge carriers recombination and poor photocatalytic stability. Therefore, there is an urgent need to develop novel photocatalysts with highly efficient and stable photoactivity.

Very recently, Li *et al.* prepared $SrSn(OH)_6$ *via* a facile homogeneous precipitation method, and the as-obtained $SrSn(OH)_6$ samples exhibited excellent UV photocatalytic performance for the degradation of benzene and rhodamine B [17]. However, to the best of our knowledge, application and reaction mechanism of $SrSn(OH)_6$ for photocatalytic removal of air pollutants has not been reported. Herein, $SrSn(OH)_6$ photocatalyst was synthesized by a facile chemical precipitation method in water bath. More importantly, this study focuses on photocatalytic NO_x removal over $SrSn(OH)_6$. Interestingly, $SrSn(OH)_6$ exhibited high photocatalytic activity and good stability in the removal of NO under the irradiation of UV light. In addition, on the basis of *in situ* DRIFTS investigations, the detailed reaction mechanism during the photocatalytic oxidation of NO_x was proposed.

Details of $SrSn(OH)_6$ synthesis, characterization method, photocatalytic activity evaluation method, and *in situ* DRIFTS investigation method (S4) are described in Supporting information.

* Corresponding authors.
E-mail addresses: zhangwendong@cqnu.edu.cn (W. Zhang), dfctbu@126.com (F. Dong).

https://doi.org/10.1016/j.cclet.2021.07.065
1001-8417/

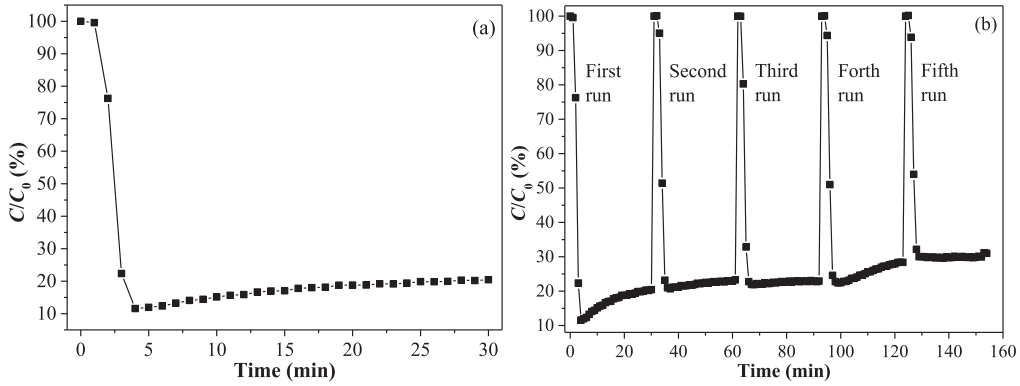

Fig. 1. (a) Photocatalytic activity and (b) recycling tests of $SrSn(OH)_6$ for NO removal under ultraviolet light irradiation (λ = 280 nm).

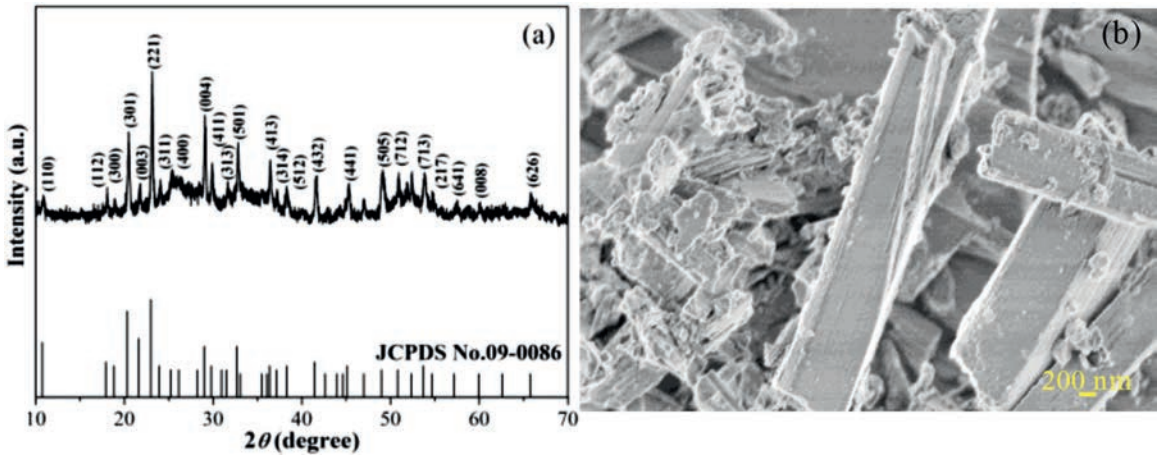

Fig. 2. (a) XRD patterns and (b) SEM image of $SrSn(OH)_6$.

As shown in Fig. 1a, the photocatalytic removal ratio of NO was up to 79.6% after ultraviolet light irradiation for 30 min with the reactive species, which is more efficient than other Bi-based and g-C_3N_4 based photocatalysts [15]. Especially, the $SrSn(OH)_6$ shows significantly higher photocatalytic activity than that of $BiOBr_{0.5}I_{0.5}$/BiOI composite (removal rate of 36.2%) [18], oxygen vacancies-mediated TiO_2 nanocrystals (removal rate of 45.0%) [19], Bi spheres/g-C_3N_4 nanohybrid (removal rate of 59.7%) [20], and defective β-Bi_2O_3 (removal rate of 52.0%) [21]. However, the concentration of generated NO_2 rises as high as 195 ppb. Actually, the NO_2 as intermediate shows more toxicity than NO, which could cause secondary pollution of atmosphere. Therefore, highly efficient inhibition of the toxic NO_2 generation should be addressed in the future work for practical application of $SrSn(OH)_6$. In addition, $SrSn(OH)_6$ only displays slight loss of photocatalytic activity even after five recycling tests (Fig. 1b). The gradual generation of intermediates and final products may occupy the active sites of $SrSn(OH)_6$, which results in the slight loss of photocatalytic activity. These results indicate that $SrSn(OH)_6$ has excellent activity and good stability during the photocatalytic removal of NO.

XRD patterns in Fig. 2a shows that all the diffraction peaks can be indexed to the hexagonal structure of $SrSn(OH)_6$ (JCPDS card No. 22-1442) [17]. As can be seen from Fig. 2b, the as-obtained $SrSn(OH)_6$ demonstrates an stick-like structure formed by stacking of large plates and particles size.

As shown in Fig. S5a (Supporting information), $SrSn(OH)_6$ featured strong light absorption in the ultraviolet light region. Moreover, the band gap energy (E_g) of $SrSn(OH)_6$ which can be determined through the plots of $(\alpha h\nu)^{1/2}$ *versus* photo energy (Fig. S5b Supporting information) is 3.53 eV. In addition, the conduction band (CB) and valence band (VB) position of $SrSn(OH)_6$ can be calculated from the relationship $E_{CB} = X - E^0 - 0.5E_g$ and $E_g = E_{VB} - E_{CB}$. Thus, the calculated E_{CB} and E_{VB} of $SrSn(OH)_6$ were 0.19 and 3.72 eV, respectively.

As shown in Figs. 3a-c, the ESR signals of $O_2^{\bullet-}$, $^{\bullet}OH$ and $^1O_2$ were increased with prolonged irradiation time, suggesting that $O_2^{\bullet-}$, $^{\bullet}OH$ and $^1O_2$ are the main active species during the photocatalytic reaction. Fig. 3d shows that photogenerated electrons can be rapidly consumed to participate in he generation of abundant active species under the ultraviolet light.

Based on the mentioned above, the valence band position of $SrSn(OH)_6$ is 3.72 eV, indicating that the hole oxidation potential of $SrSn(OH)_6$ is much higher than those of $OH^-/^{\bullet}OH$ (1.99 eV) and $H_2O/^{\bullet}OH$ (2.37 eV). Therefore, the $^{\bullet}OH$ radicals could be directly generated from the oxidation of OH^- (Eq. 1) or H_2O (Eq. 2). And besides, the conduction band position of $SrSn(OH)_6$ is only 0.19 eV, hence, the e^- reduction potential of $SrSn(OH)_6$ is obviously more positive than that of $O_2/O_2^{\bullet-}$ (–0.33 eV). Thus, the e^- reduction potential of $SrSn(OH)_6$ could not directly reduce O_2 to $O_2^{\bullet-}$ radicals. The main active species can be formed through a series of reactions as follows: Eqs. 1-6. Especially, the $^1O_2$ radicals can be produced by the further oxidation of $O_2^{\bullet-}$ radicals with photogenerated holes (Eq. 5) [22].

$$OH^- + h^+ \rightarrow {}^{\bullet}OH \quad (1)$$

$$H_2O + h^+ \rightarrow {}^{\bullet}OH + H^+ \quad (2)$$

$$^{\bullet}OH + {}^{\bullet}OH \rightarrow H_2O_2 \quad (3)$$

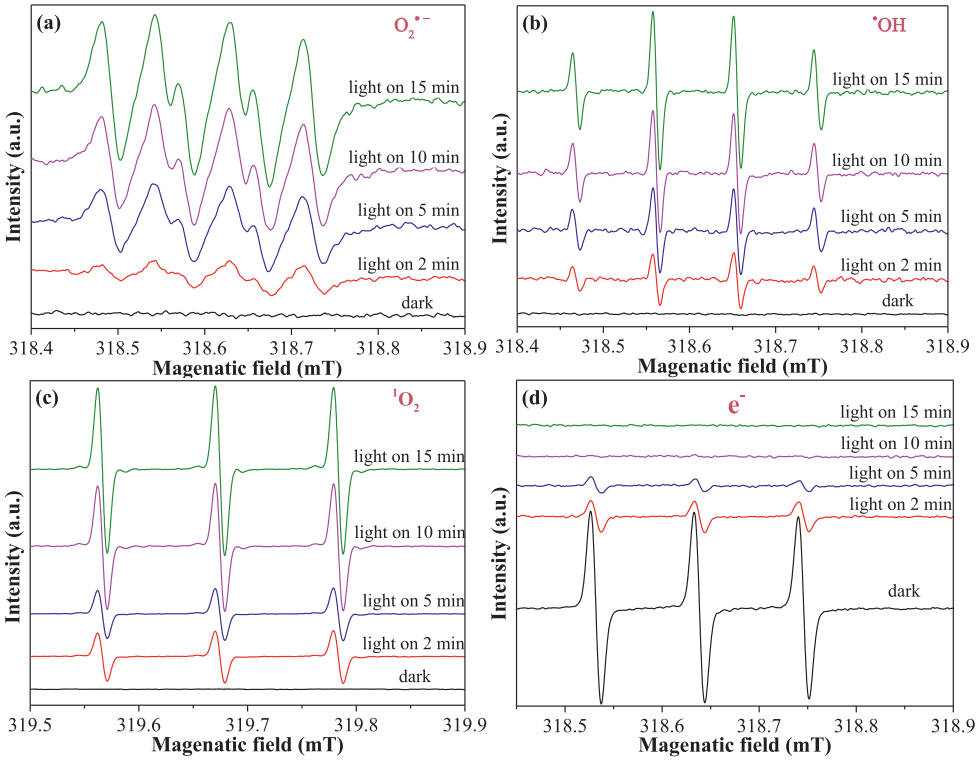

Fig. 3. ESR spectra of radical adduct trapped by (a) DMPO-$O_2^{\bullet-}$, (b) DMPO-•OH, (c) 4-oxo-TEMP-$^1O_2$ and (d) TEMPO-e^- over $SrSn(OH)_6$ under ultraviolet irradiation (λ = 280~360 nm).

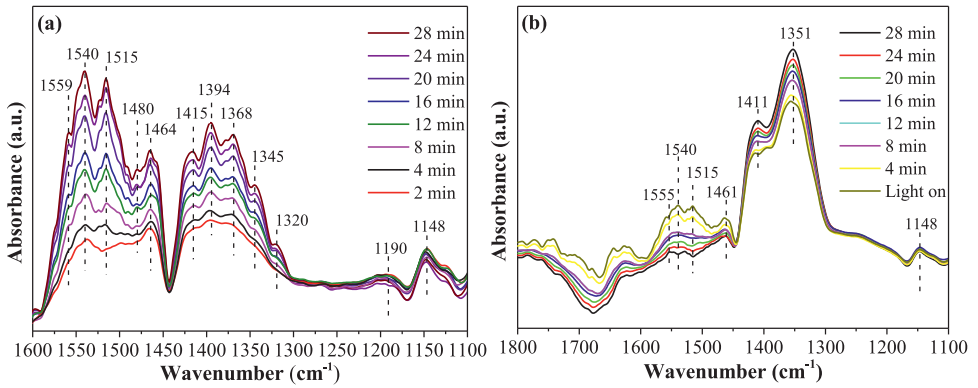

Fig. 4. *In situ* DRIFTS spectra of the adsorption (a) and photocatalytic removal (b) of NO on the surface of $SrSn(OH)_6$.

$$H_2O_2 + h^+ \rightarrow O_2^{\bullet-} + 2H^+ \quad (4)$$

$$O_2^{\bullet-} + h^+ \rightarrow {}^1O_2 \quad (5)$$

Fig. 4a shows *in situ* DRIFTS spectra of the adsorption of NO on the surface of $SrSn(OH)_6$. The peaks at 1148 and 1190 cm^{-1} can be assigned to the original NO. The peaks at 1320, 1345, 1368, 1394 and 1415 cm^{-1} can be assigned to NO_2, which is the preliminary oxidation product during the adsorption process (Eq. 6). The peaks at 1464 cm^{-1} can be assigned to NO_2^-, other peaks at 1480, 1515, 1540 and 1559 cm^{-1} can be attributed to NO_3^-, which is the subsequent reaction product of NO_2 and H_2O (Eq. 7). These results indicate that the NO_2, NO_2^- and NO_3^- yield increased rapidly during the adsorption stage in the NO and O_2 environment [23,24].

$$2NO + O_2 \rightarrow 2NO_2 \quad (6)$$

$$2NO_2 + H_2O \rightarrow HNO_3 + HNO_2 \quad (7)$$

After the light was turned on Fig. 4b), a new peak appeared rapidly at 1351 cm^{-1} during the irradiation process, which is regarded as the oxidation of NO_2 and NO into NO_3^- by •OH, $O_2^{\bullet-}$ and $^1O_2^-$ radicals (Eqs. 8-11. In addition, the hole oxidation potential of $SrSn(OH)_6$ is higher than those of $E_{\varphi HNO_3/NO}$ (0.94 eV *vs.* NHE), $E_{\varphi HNO_2/NO}$ (0.99 eV *vs.* NHE), and $E_{\varphi NO_2/NO}$ (1.03 eV *vs.* NHE); hence, the photo-generated holes of $SrSn(OH)_6$ could directly oxidize NO to NO_2, NO_2^- and NO_3^- (Eq. 12). As the illumination time was prolonged, the intensities of the peaks at 1515, 1540 and 1555 cm^{-1} gradually decreased. However, the new peak (1411 cm^{-1}) of NO_2 gradually became stronger, which reflects the high yield of NO_2 owing to the reaction of NO_3^- and NO (Eq. 13) [25-26].

$$NO_2 + e^- \rightarrow NO_2^- \quad (8)$$

$$NO_2^- + 2{}^{\bullet}OH \rightarrow NO_3^- + H_2O \quad (9)$$

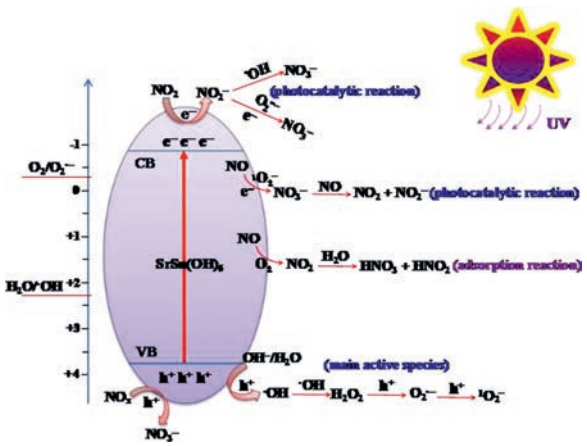

Fig. 5. The proposed photocatalytic NO oxidation mechanisms.

$$2NO_2^- + O_2^{\bullet-} + e^- \rightarrow 2NO_3^- \quad (10)$$

$$NO + {}^1O_2^- + e^- \rightarrow NO_3^- \quad (11)$$

$$NO_x + h^+(SrSn(OH)_6) \rightarrow NO_3^- \quad (12)$$

$$NO_3^- + NO \rightarrow NO_2 + NO_2^- \quad (13)$$

Based on the ESR and the *in situ* DRIFTS results, the photocatalytic NO oxidation mechanisms were provided in Fig. 5. The roles of $O_2^{\bullet-}$, $^{\bullet}OH$ and $^1O_2$ in NO oxidation were illustrated.

In summary, the $SrSn(OH)_6$ photocatalyst with stick-like structure was synthesized by a simple chemical precipitation method in water bath. The as-obtained $SrSn(OH)_6$ exhibited excellent photocatalytic activity and good stability. Interestingly, it was found that $SrSn(OH)_6$ photocatalyst demonstrated the ability to generate the main active species of $O_2^{\bullet-}$, $^{\bullet}OH$ and $^1O_2$ and could oxidize NO into nitrate. To clarify the adsorption and reaction mechanism, the intermediates and final products that distributed on the surface of $SrSn(OH)_6$ were determined and analyzed by *in situ* DRIFTS. And thus the photocatalytic NO oxidation mechanism on $SrSn(OH)_6$ was proposed. The present work could provide new insights into the $SrSn(OH)_6$ with high activity for photocatalytic NO_x removal.

Declaration of competing interest

The authors declare that they have no known competing financial interests or personal relationships that could have appeared to influence the work reported in this paper.

Acknowledgments

This research is financially supported by the National Natural Science Foundation of China (No. 51708078), the Science and Technology Research Program of Chongqing Municipal Education Commission (No. KJZD-K201900502), and the Natural Science Foundation of Chongqing (No. 2018jcyjA1040), the Innovative Research Team of Chongqing (No. CQYC201903221).

Supplementary materials

Supplementary material associated with this article can be found, in the online version, at doi:10.1016/j.cclet.2021.07.065.

References

[1] R. Sarath, S. Trishul, M. Meredith, et al., Clin. Chest. Med. 41 (2020) 825–843.
[2] M.W. Tessum, L. Sheppard, T.V. Larson, et al., Environ. Sci. Technol. 55 (2021) 3530–3538.
[3] X. Lu, S. Zhang, J. Xing, et al., Engineering 6 (2020) 1423–1431.
[4] J. Wu, Y. Zhang, T. Wang, et al., Atmos. Pollut. Res. 11 (2020) 693–701.
[5] Z. Zhou, Y. Li, M. Li, et al., Chin. Chem. Lett. 30 (2019) 2698–2704.
[6] C. Yuan, W. Cui, Y. Sun, et al., Chin. Chem. Lett. 31 (2020) 751–754.
[7] Y. Zheng, Z. Pan, X. Wang, Chin. J. Catal. 34 (2013) 524–535.
[8] Q. Lu, Y. Yu, Q. Ma, et al., Adv. Mater. 28 (2016) 1917–1933.
[9] X. Meng, Z. Zhang, J. Mol. Catal. A: Chem. 423 (2016) 533–549.
[10] H.L. NguYen, Adv. Energy Mater. 10 (2020) 2002091.
[11] S. Chu, Y. Wang, C. Wang, et al., Int. J. Hydrogen Energy 38 (2013) 10768–10772.
[12] S. Cao, J. Low, J. Yu, et al., Adv. Mater. 27 (2015) 2150–2176.
[13] S. Ghosh, N.A. Kouamé, L. Ramos, et al., Nat. Mater. 14 (2015) 505–511.
[14] G. Liu, P. Niu, H. Cheng, ChemPhysChem 14 (2013) 885–892.
[15] F. Dong, T. Xiong, Y. Sun, et al., Chem. Commun. 50 (2014) 10386–10389.
[16] Z. Zhao, Zhang W, X. Lv, et al., Environ. Sci. Nano. 3 (2016) 1306–1317.
[17] Y. Luo, J. Chen, J. Liu, et al., Appl. Catal. B: Environ. 182 (2015) 533–540.
[18] M. Kou, Y. Deng, R. Zhang, et al., Chin. J. Catal. 41 (2020) 1480–1487.
[19] Z. Gu, Z. Cui, Z. Wang, et al., J. Catal. 393 (2021) 179–189.
[20] F. Dong, Z. Zhao, Y. Sun, et al., Environ. Sci. Technol. 49 (2015) 12432–12440.
[21] B. Lei, W. Cui, J. Sheng, et al., Sci. Bull. 65 (2020) 467–476.
[22] Y. Nosaka, A. Nosaka, Chem. Rev. 117 (2017) 11302–11336.
[23] H. Liu, H. Mei, N. Miao, et al., Chem. Eng. J. 414 (2021) 128748.
[24] S. Luo, X. Liu, X. Wei, et al., J. Hazard. Mater. 399 (2020) 122824.
[25] H. Wang, W. Zhang, X. Li, et al., Appl. Catal. B: Environ. 225 (2018) 218–227.
[26] W. He, X. Wu, Y. Li, et al., Chin. Chem. Lett. 31 (2020) 2774–2778.